DYNAMIC STABILITY

By Leonard Sternfield

Langley Aeronautical Laboratory

The problem of dynamic stability of airplanes is concerned with the motion of an airplane following a disturbance from an initial condition of equilibrium. Such disturbances may be caused by sudden gusts of wind or by deflection of the control surfaces. If the motion of the airplane caused by the disturbance damps, the airplane is said to be dynamically stable; if the motion caused by the disturbance builds up, the airplane is dynamically unstable. The mode of motion which may characterize dynamic instability is either an aperiodic divergence or an unstable oscillation. For many airplanes, the divergence of the aperiodic mode occurs at a slow rate and therefore pilots do not find this type of instability troublesome; hence, these airplanes are considered satisfactory, from the dynamic-stability viewpoint, even though the aperiodic mode is divergent. The oscillatory mode, however, may be objectionable to the pilot despite the fact that the oscillation is stable. The present paper on dynamic stability, therefore, will be mainly concerned with the oscillatory mode of motion.

The general equations of motion representing the motion of an airplane are referred to a system of axes which are fixed in the airplane and move with it. A system of axes that is commonly used by NACA authors is known as the stability system of axes. (See fig. 1.) The stability axes constitute an orthogonal system of axes having its origin at the center of gravity and in which the Z-axis is in the plane of symmetry and perpendicular to the relative wind, the X-axis is in the plane of symmetry and perpendicular to the Z-axis, and the Y-axis is perpendicular to the plane of symmetry. An equation of motion referred to these axes is set up for each one of the six degrees of freedom. Three of the equations are obtained by equating the aircraft mass accelerations along each axis to the aerodynamic forces and the other three equations are obtained by equating the rate of change of moment of momentum about each axis to the aerodynamic moments. (See references 1 to 4.)

A complete treatment of the dynamic stability of airplanes using the six equations would be extremely lengthy and very complex. Certain simplifying assumptions have therefore been made to facilitate the analysis. Since the airplane is symmetrical with respect to the plane that includes the fuselage axis and is perpendicular to the span axis and the steady motion about which the disturbances occur is symmetrical with regard to that plane, the six equations can be separated into a symmetric or longitudinal group consisting of three equations and an asymmetric or lateral group consisting of the other three equations, with no coupling between the two groups. The dynamic-stability investigation is therefore divided into two parts, a lateral-stability analysis and a longitudinal-stability analysis. The second assumption consists of the

application of the theory of small oscillations to both lateral and longitudinal stability, which means that second—order terms are neglected. The third assumption is that the aerodynamic forces depend solely upon the instantaneous motion of the airplane and not upon the rate at which the motion is changing. That is, it is assumed that when the angle of attack of the wing changes suddenly from one steady value to another, the lift changes instantaneously — although actually the lift approaches asymptotically the value corresponding to the new angle of attack.

The general methods involved in a dynamic—stability investigation will be presented for the lateral—stability analysis but a similar procedure is also applicable to the longitudinal—stability analysis. The linearized equations of motions, referred to the stability axes, used in the lateral-stability analysis for the condition of controls fixed are as follows:

Roll

$$2\mu_b\left(K_X^2 D_b^2\phi + K_{XZ}D_b^2\psi\right) = C_{l_\beta}\beta + \frac{1}{2}C_{l_p}D_b\phi + \frac{1}{2}C_{l_r}D_b\psi$$

Yaw

$$2\mu_b\left(K_Z^2 D_b^2\psi + K_{XZ}D_b^2\phi\right) = C_{n_\beta}\beta + \frac{1}{2}C_{n_p}D_b\phi + \frac{1}{2}C_{n_r}D_b\psi$$

Sideslip

$$2\mu_b\left(D_b\beta + D_b\psi\right) = C_{Y_\beta}\beta + \frac{1}{2}C_{Y_p}D_b\phi + C_L\phi + \frac{1}{2}C_{Y_r}D_b\psi + \left(C_L \tan\gamma\right)\psi$$

An equation of motion is presented for each one of the three degrees of freedom involved in lateral motion: roll, yaw, and sideslip. On the left—hand side of the equations are written the moment of inertia and product of inertia times the acceleration and on the right—hand side are written the aerodynamic forces or moments expressed as stability derivatives. These equations are linear differential equations with constant coefficients and, therefore, the solution of the equations of motion follows the usual procedure for linear differential equations. When $\phi_0 e^{\lambda s}$ is substituted for ϕ, $\psi_0 e^{\lambda s}$ for ψ, and $\beta_0 e^{\lambda s}$ for β in the equations written in determinant form, λ must be a root of the equation

$$A\lambda^4 + B\lambda^3 + C\lambda^2 + D\lambda + E = 0$$

Where the coefficients A, B, C, D, and E are functions of the mass and aerodynamic parameters of the equations. The roots of this stability equation determine the modes of motion. A real root indicates an aperiodic

mode and a complex root indicates an oscillatory mode. The signs of the
roots determine the stability of the system. If the real roots are
negative and the real part of the complex roots is negative, the airplane
is dynamically stable. If any one of the real roots is positive or the
real part of the complex root is positive, the airplane is dynamically
unstable. The conditions for complete stability (reference 5) are
that all the coefficients of the stability equation and the
discriminant $R = BCD - AD^2 - B^2E$, known as Routh's discriminant, be
positive. However, as mentioned previously, the mode which is of parti-
cular interest is the oscillatory mode. The first step in the analysis
of the oscillatory mode is to determine the boundary for neutral oscill-
atory stability. This boundary is usually plotted as a function of two
of the most important stability derivatives affecting lateral stability —
the directional stability parameter C_{n_β}, which expresses the variation

of yawing-moment coefficient with sideslip, and the effective dihedral
derivative C_{l_β}, which expresses the variation of the rolling-moment

coefficient with sideslip. The necessary and sufficient conditions for
neutral oscillatory stability are that the coefficients of the stability
equation satisfy Routh's discriminant set equal to zero and that the B-
and D-coefficients have the same sign. (See reference 5.) The lateral-
stability boundaries for a high-speed airplane are given in figure 2(a).
The ordinate in this figure is C_{n_β}' and the abscissa is C_{l_β}. The solid

boundary labeled $R = 0$ is the boundary for neutral oscillatory stability.
This boundary divides the quadrant into a stable and unstable region. For
example, for combinations of C_{n_β} and C_{l_β} located below this boundary,

that is, on the shaded side of the boundary, the oscillation of the airplane
is unstable. The dashed boundary labeled $R = 0$ satisfies the condition
that Routh's discriminant is zero but violates the condition that the B-
and D-coefficients must be of the same sign, because the B-coefficient is
positive and the D-coefficient is negative for combinations of C_{n_β}
and C_{l_β} below the boundary $D = 0$. Hence this curve $R = 0$ is not a

neutral-oscillatory boundary. The curve obtained by setting the E-
coefficient equal to zero is known as the spiral-stability boundary. This
boundary determines the stability of the numerically small real root, known
as the spiral mode. For combinations of C_{n_β} and C_{l_β} on the shaded side

of the line $E = 0$, the airplane is spirally unstable. There is one more
mode which usually occurs in lateral motion. This mode corresponds to the
heavy damping of the rolling motion due to the damping-in-roll derivative C_{l_p}.

In general, therefore, the four roots obtained from the lateral-stability
equation usually consist of one conjugate complex pair and two real roots.
For some airplane configurations, both branches of $R = 0$ are true
neutral-oscillatory-stability boundaries, as shown in figure 2(b). The
significance of the two boundaries can best be understood by analyzing
the modes of motion for combinations of C_{n_β} and C_{l_β} represented by

the points (A), (B), (C), (D), and (E) in this figure. At point (A),

the roots of the stability equation are two negative real roots and one conjugate complex pair with the real part negative. Hence, the airplane is dynamically stable. Passing through the boundary $E = 0$ to point (B) causes one of the real roots to change sign, which indicates that the airplane is dynamically unstable because of spiral instability. Upon crossing the boundary $R = 0$ to point (C), the real part of the complex root changes sign as expected, which indicates that the oscillatory mode is unstable. Thus far, the roots consisted of two real roots and one conjugate complex pair. At point (D), however, the solution of the stability equation results in two pairs of complex roots with the real part of each pair of roots negative. The period of the oscillation which corresponds to one pair of the complex roots is about the same order of magnitude as the period of the oscillation at points (A), (B), (C) — approximately 3 seconds. The period of the other oscillation is much greater — for some airplanes, the period of this oscillation is of the order of magnitude of 15 seconds. It is this long—period oscillation which becomes unstable upon crossing the boundary $R = 0$ from point (D) to point (E). That is, at point (E) two pairs of complex roots are obtained with a positive real part of the complex roots that corresponds to the long—period oscillation so that an unstable oscillation is indicated, and a negative real part of the complex roots that corresponds to the short-period oscillation so that a stable oscillation is indicated. Thus the two curves for $R = 0$ represent neutral—oscillatory—stability boundaries, one boundary for the long—period oscillation and the other boundary for the short—period oscillation.

The second step in the analysis of the oscillatory mode is to determine the relation between the period and damping of the oscillation in the stable region. As mentioned previously, a pair of complex roots indicates an oscillatory mode. The real part of a complex root gives the damping factor and the imaginary part of the complex root gives the angular frequency of the oscillation from which the period is computed. A convenient measure of the damping is the time required for the amplitude of a disturbance to damp to half amplitude. The ratio of the time required to damp to half amplitude to the period results in the number of cycles required to damp to half amplitude. Figure 3 shows the curves of constant period and constant damping for a hypothetical airplane plotted as a function of C_{n_β} and C_{l_β}. (See reference 6.) The values corresponding to the solid curves represent the time in seconds to damp to half amplitude. As this time increases, the damping of the oscillation decreases. The solid curve labeled ∞ is the neutral-oscillatory—stability boundary; combinations of C_{n_β} and C_{l_β} located below this boundary will result in an unstable oscillation. The period of the oscillation in seconds is indicated by the values corresponding to the dashed curves. There are, at present, two schools of thought on the question as to which region in the C_{n_β}, C_{l_β} plane would result in a more satisfactory type of oscillation. For example, if the values of C_{n_β} and C_{l_β} for a given airplane correspond to point A and it is desired to improve the relation between the period and damping of the

oscillation, one group is of the opinion that the weathercock stability of the airplane should be increased. Thus, in going from (A) to (B), the damping of the oscillation is increased from 16 seconds to damp to half amplitude at (A) to 6 seconds at (B). But the period is shortened, thereby causing the number of cycles to damp to half amplitude to increase from 4 cycles at (A) to 6 cycles at (B). For this modification in the design of the airplane, therefore, the damping in seconds is improved but the damping in cycles is worsened. The opinion of the other group is that the combinations of C_{n_β} and C_{l_β} should be restricted to a small region near the origin, from point (A) to point (C). The damping in seconds is now reduced but because the period is lengthened the damping in cycles is improved, from 4 cycles at (A) to 1.67 cycles at (C). It is apparent that the desired criterion cannot be determined by the dynamic-stability investigator but must be based upon the opinions of pilots from more extensive flight-test results. Once this criterion is established, however, a figure similar to figure 3 which shows the curves of constant period and constant damping is necessary to indicate the possible combinations of C_{n_β} and C_{l_β} that will satisfy the criterion.

The dynamic-stability calculations have thus far yielded only an indication of the character of the free motion. The motion of the airplane, subsequent to a disturbance from its trimmed condition, is compounded of the several modes of motion in different proportions. The motion can be calculated by applying the Heaviside Operational Calculus or the Laplace transform to the equation of motion. The Laplace transform is considered a more powerful method than the Heaviside method because the initial conditions of the problem, initial displacements or initial velocities, are inherently taken into account by the Laplace transform. The application of these methods to the calculation of airplane motions can be found in several NACA and British reports. (See references 7 to 11.)

The present discussion has thus far been mainly concerned with the general methods of dynamic-stability analysis. The effects of some of the more important mass and aerodynamic parameters on the lateral stability will now be illustrated by showing the relative location of the neutral-oscillatory-stability boundaries in the C_{n_β}, C_{l_β} plane as these mass and aerodynamic parameters are varied.

Until recently, the product-of-inertia effect, which results from the inclination of the principal longitudinal axis of inertia relative to the flight path, has usually been neglected in lateral-stability analyses because some calculations for conventional airplanes had indicated that to neglect the angularity of the principal longitudinal axis to the flight path did not seriously affect the lateral stability. (See reference 12.) The angularity of the principal axis relative to the flight path causes the inertia forces to produce a coupling between the rolling and yawing motions so that a rolling acceleration produces a yawing moment and a yawing acceleration produces a rolling moment. Recent studies have shown, however, that the product of inertia may have a very pronounced

effect on the lateral stability of present-day airplanes designed for high-speed high-altitude flight because of high wing loadings, large differences between rolling and yawing moments of inertia, and the aerodynamic characteristics of low-aspect-ratio or swept wings. (See references 13 to 15.)

There has been a trend in the design of recent high-speed airplanes toward the use of relatively large angles of wing incidence to permit the fuselage to remain at a low angle of attack while the wing goes up to the high angles of attack required because of the high sweep and low aspect ratio. The purpose in designing the airplane so that the fuselage remains at a small angle of attack is to reduce the fuselage drag for high altitude or cruising flight or to reduce the fuselage ground angle and thereby simplify the landing-gear design. The important factor to consider in analyzing the effect of wing incidence on the lateral oscillatory stability is the inclination of the principal longitudinal axis relative to the flight path. Figure 4 shows the calculated oscillatory-stability boundaries as a function of C_{n_β} and C_{l_β} for a model tested in the Langley free-flight tunnel with the wing set at two angles of incidence, $i_w = 0°$ and $i_w = 10°$. In each of these configurations the model was flown at the same lift coefficient which corresponded to an angle of attack of $10°$ for the wing. The results indicate that when the wing was set at $0°$ incidence, both the wing and the principal longitudinal axis of the model, which coincided with the fuselage reference axis, were inclined $10°$ above the flight path to obtain the lift coefficient for trim. For that condition, illustrated by the lower sketch in the figure, the boundary falls in the lower region of the quadrant; thus, oscillatory stability is indicated for a large number of combinations of C_{n_β} and C_{l_β} located above the boundary. However, if the wing is set at an angle of incidence to obtain lift (for this case $10°$), as has been proposed in several designs, and the principal axis is alined along the flight path, the oscillatory boundary falls in the upper region of the quadrant and thus it is very difficult to obtain oscillatory stability because the stable combinations of C_{n_β} and C_{l_β} are limited to the small region above this boundary. The stabilizing shift in the boundary, from $i_w = 10°$ to $i_w = 0°$, is caused by the fact that the principal longitudinal axis is inclined $10°$ above the flight path for $i_w = 0°$. The boundaries indicate that the model with values of C_{n_β} and C_{l_β} shown by the test point on the figure, that is, C_{n_β} about 0.0025 and C_{l_β} approximately -0.003, is stable when the incidence is $0°$ and unstable when the incidence is $10°$. This fact was verified by flight tests of the model in the Langley free-flight tunnel. (See reference 14.)

The important effect of the product of inertia on the oscillatory stability is emphasized by figure 5. The boundaries presented in this figure are for a high-speed airplane with a wing loading of 70 pounds

per square foot cruising at an altitude of 30,000 feet. The boundaries are again plotted as a function of C_{n_β} and C_{l_β} for two cases: The upper boundary represents the case in which the principal axis is inclined at an angle of 2° below the flight path at the nose, $\eta = -2^\circ$, and the lower boundary represents the case in which the principal axis is alined with the flight path, $\eta = 0^\circ$. A comparison of the two boundaries shows a large destabilizing shift in the boundary as the principal axis falls below the flight path. That is, as the boundary shifts upward from $\eta = 0^\circ$ to $\eta = -2^\circ$, the stable region located above the boundary is reduced. Such a marked shift in the boundary is caused by only 2° variation in the inclination of the principal longitudinal axis to the flight path.

The effect of wing loading and altitude on the oscillatory-stability boundary is illustrated by figure 6. The effects of these two parameters are treated simultaneously by considering variation in the relative-density factor μ_b, the ratio of the airplane density to air density, since this factor varies directly with both wing loading and altitude. The boundaries are shown for various values of μ_b. The values of μ_b can be interpreted in terms of wing loading and altitude as follows: A value of μ_b of 5 corresponds to a light plane with a wing loading of 10 pounds per square foot at an altitude of 10,000 feet; a value of μ_b of 30 corresponds to a World War II fighter with a wing loading of 40 pounds per square foot at an altitude of 40,000 feet; and a value μ_b of 1000 would correspond to a postwar high-speed design airplane with a wing loading of 100 pounds per square foot flying at an altitude of 60,000 feet. It is apparent from this figure that an increase in wing loading or altitude, or an increase in μ_b, shifts the boundaries upward so that a decrease in the stable region is indicated. However, it is important to note that the most pronounced effect of wing loading and altitude on stability occurs for values of μ_b less than 30, in the range of light aircraft design, whereas for values of μ_b above 30, wing loading and altitude have very little effect on stability. (See reference 16.)

One of the most important stability derivatives affecting lateral stability is the damping-in-roll derivative C_{l_p}, which becomes smaller as the sweepback is increased and as the aspect ratio is decreased. Figure 7 shows the effect of C_{l_p} on the oscillatory-stability boundary. The boundaries are plotted for several values of C_{l_p}: 0, -0.1, and -0.2. The value of C_{l_p} for a straight-wing conventional airplane is about -0.4 or -0.5. These boundaries were calculated for a hypothetical transonic airplane and are intended only to indicate the trends obtained as C_{l_p} is varied. It is evident from the boundaries that reducing C_{l_p} reduced

the lateral stability. Although the effect shown is typical for most airplane designs, calculations have indicated that the reverse effect might be present for some airplane configurations. The effect of some of the other stability derivatives and mass characteristics on the lateral oscillatory stability are presented in several NACA reports. (See references 15 and 17 to 19.)

The dynamic longitudinal stability of airplanes with controls fixed has received very extensive treatment by many authors, among whom may be mentioned Bryan, Bairstow, Wilson, and Zimmerman. (See references 1 to 3 and 20 to 22.) In general, the longitudinal motion consists of two oscillatory modes — a slightly damped long-period oscillation, known as the phugoid, and a heavily damped short-period oscillation. Because of the relation between the period and damping of each one of the oscillations, the longitudinal stability of most airplanes has been satisfactory to the pilots.

An analysis of lateral or longitudinal motion of the airplane with controls free involves an equation for an additional degree of freedom, that is, for the motion of the control itself. The discussion of control-free stability will be mainly concerned with the rudder-free case, although similar analyses have been carried out for the case of elevator free and aileron free. (See references 23 to 28.) Flight tests have shown that, under certain conditions of rudder balance, undamped lateral oscillations may occur when the rudder is freed. The oscillations involve coupling between the yawing motions of the airplane and movements of the rudder and depend on the amount of friction in the control system. Two of the most important parameters affecting the control-free stability are the restoring moment parameter C_{h_δ}, which expresses the variation of

rudder hinge-moment coefficient with rudder deflection, and the floating-moment parameter C_{h_ψ}, which expresses the variation of the hinge-moment

coefficient with the angle of yaw. Figure 8 shows the calculated rudder-free-stability boundaries with the effect of friction in the control system taken into account. These boundaries are plotted with C_{h_δ} as

abscissa and C_{h_ψ} as ordinate. Positive values of C_{h_ψ} correspond to

positive floating tendency, that is, surfaces whose free movements tend to oppose any disturbance of the airplane. The boundaries indicate that, for combinations of C_{h_δ} and C_{h_ψ} located on the shaded side of $R = 0$,

the oscillation is unstable. If there is no solid friction in the system, the completely stable region is between $R = 0$ and the divergence boundary. However, if there is solid friction in the system, constant-amplitude oscillations occur for combinations of C_{h_δ} and C_{h_ψ} located

between $R = 0$ and the curve labeled "friction boundary." The amplitude of the steady oscillation is proportional to the amount of solid friction in the control system. Flight tests will be necessary to indicate the maximum amount of steady oscillation that is allowable in an airplane.

The present paper indicates in general the effect of some of the mass and aerodynamic parameters on the lateral oscillatory stability. The results are illustrated for an airplane or model with a given set of values of mass and aerodynamic parameters. However, as shown in more complete lateral—stability studies, small variations in some of these parameters may cause a pronounced change in the oscillatory stability. On the basis of these detailed studies, therefore, it appears necessary to make a separate stability analysis for each airplane.

Some of the subjects that require further theoretical or experimental research are:

1. The effects of the aeroelasticity of wings on stability derivatives and hence on dynamic stability

2. The effects of power on stability

3. Analysis of the snaking or lightly damped short—period oscillations encountered recently in high—speed flight

4. Stability derivatives for transonic region

5. Analysis to determine important combinations of mass and aerodynamic parameters which affect dynamic stability

APPENDIX

SYMBOLS AND COEFFICIENTS

ϕ angle of bank, radians

ψ angle of azimuth, radians

β angle of sideslip, radians $\left(\dfrac{v}{V}\right)$

v sideslip velocity along the Y-axis, feet per second

V airspeed, feet per second

ρ mass density of air, slugs per cubic foot

q dynamic pressure, pounds per square foot $\left(\dfrac{1}{2}\rho V^2\right)$

b wing span, feet

S wing area, square feet

W weight of airplane, pounds

m mass of airplane, slugs $\left(\dfrac{W}{g}\right)$

g acceleration due to gravity, feet per second per second

μ_b relative-density factor $\left(\dfrac{m}{\rho S b}\right)$

η angle of attack of principal longitudinal axis of airplane, positive when principal axis is above flight path, degrees

γ angle between flight path and horizontal axis, positive in a climb, degrees

k_{X_o} radius of gyration in roll about principal longitudinal axis, feet

k_{Z_o} radius of gyration in yaw about the principal vertical axis, feet

K_{X_o} nondimensional radius of gyration in roll about principal longitudinal axis $\left(\dfrac{k_{X_o}}{b}\right)$

K_{Z_o} nondimensional radius of gyration in yaw about principal vertical axis $\left(\dfrac{k_{Z_o}}{b}\right)$

K_X nondimensional radius of gyration in roll about longitudinal stability axis $\left(\sqrt{K_{X_o}{}^2 \cos^2\eta + K_{Z_o}{}^2 \sin^2\eta}\right)$

K_Z nondimensional radius of gyration in yaw about vertical stability axis $\left(\sqrt{K_{Z_o}{}^2 \cos^2\eta + K_{X_o}{}^2 \sin^2\eta}\right)$

K_{XZ} nondimensional product-of-inertia parameter $\left(\left(K_{Z_o}{}^2 - K_{X_o}{}^2\right)(\sin\eta \cos\eta)\right)$

t time, seconds

S_b distance along flight path, in spans $\left(\dfrac{Vt}{b}\right)$

D_b differential operator $\left(\dfrac{d}{dS_b}\right)$

C_L trim lift coefficient $\left(\dfrac{W \cos\gamma}{qS}\right)$

C_l rolling-moment coefficient $\left(\dfrac{\text{Rolling moment}}{qSb}\right)$

C_n yawing-moment coefficient $\left(\dfrac{\text{Yawing moment}}{qSb}\right)$

C_Y lateral-force coefficient $\left(\dfrac{\text{Lateral force}}{qS}\right)$

C_{l_β} effective-dihedral derivative, rate of change of rolling-moment coefficient with angle of sideslip, per radian in equations and per degree in figures $\left(\dfrac{\partial C_l}{\partial \beta}\right)$

C_{n_β} directional-stability derivative, rate of change of yawing-moment coefficient with angle of sideslip, per radian in equations and per degree in figures $\left(\dfrac{\partial C_n}{\partial \beta}\right)$

C_{Y_β} lateral-force derivative, rate of change of lateral-force coefficient with angle of sideslip, per radian $\left(\dfrac{\partial C_Y}{\partial \beta} \right)$

C_{n_r} damping-in-yaw derivative, rate of change of yawing-moment coefficient with yawing-angular-velocity factor, per radian $\left(\dfrac{\partial C_n}{\partial \dfrac{rb}{2V}} \right)$

C_{n_p} rate of change of yawing-moment coefficient with rolling-angular-velocity factor, per radian $\left(\dfrac{\partial C_n}{\partial \dfrac{pb}{2V}} \right)$

C_{l_p} damping-in-roll derivative, rate of change of rolling-moment coefficient with rolling-angular-velocity factor, per radian $\left(\dfrac{\partial C_l}{\partial \dfrac{pb}{2V}} \right)$

C_{l_r} rate of change of rolling-moment coefficient with yawing-angular-velocity factor, per radian $\left(\dfrac{\partial C_l}{\partial \dfrac{rb}{2V}} \right)$

C_{Y_p} rate of change of lateral-force coefficient with rolling-angular-velocity factor, per radian $\left(\dfrac{\partial C_Y}{\partial \dfrac{pb}{2V}} \right)$

C_{Y_r} rate of change of lateral-force coefficient with yawing-angular-velocity factor, per radian $\left(\dfrac{\partial C_Y}{\partial \dfrac{rb}{2V}} \right)$

REFERENCES

1. Bairstow, Leonard: Applied Aerodynamics. Longmans, Green and Co., 1920.

2. Bryan, G. H.: Stability in Aviation. Macmillan and Co., Ltd., 1911.

3. Wilson, Edwin Bidwell: Aeronautics. John Wiley and Sons, Inc., 1920.

4. Jones, B. Melvill: Dynamics of the Airplane. Vol. V of Aerodynamic Theory, div. N., W. F. Durand, ed., Julius Springer (Berlin), 1935.

5. Routh, Edward John: Dynamics of a System of Rigid Bodies. Part II. 6th ed., rev. and enl., Macmillan and Co., Ltd., 1905, p. 223.

6. Brown, W. S.: A Simple Method of Constructing Stability Diagrams. R. & M. No. 1905, British A.R.C., 1942.

7. Jones, Robert T.: A Simplified Application of the Method of Operators to the Calculation of Disturbed Motions of an Airplane. NACA Rep. No. 560, 1936.

8. Jones, Robert T.: Calculation of the Motion of an Airplane under the Influence of Irregular Disturbances. Jour. Aero. Sci., vol. 3, no. 12, Oct. 1936, pp. 419-425.

9. Jones, Robert T.: The Influence of Lateral Stability on Disturbed Motions of an Airplane with Special Reference to the Motions Produced by Gusts. NACA Rep. No. 638, 1938.

10. Bryant, L. W., and Williams, D. H.: The Application of the Method of Operators to the Calculation of the Disturbed Motion of an Aeroplane. R. & M. No. 1346, British A.R.C., 1931.

11. Gandy, R. W.: The Response of an Aeroplane to the Application of Ailerons and Rudders. Part I — Response in Roll. R. & M. No. 1915, British A.R.C., 1943.

12. Zimmerman, C. H.: An Analysis of Lateral Stability in Power-Off Flight with Charts for Use in Design. NACA Rep. No. 589, 1937.

13. Sternfield, Leonard: Effect of Product of Inertia on Lateral Stability NACA TN No. 1193, 1947.

14. McKinney, Marion O., Jr., and Drake, Hubert M.: Correlation of Experimental and Calculated Effects of Product of Inertia on Lateral Stability. NACA TN No. 1370, 1947.

15. Sternfield, Leonard: Some Considerations of the Lateral Stability of High-Speed Aircraft. NACA TN No. 1282, 1947.

16. Campbell, John P., and Seacord, Charles L., Jr.: Effect of Wing
    Loading and Altitude on Lateral Stability and Control Characteristics
    of an Airplane as Determined by Tests of a Model in the Free-Flight
    Tunnel. NACA ARR No. 3F25, 1943.

17. Campbell, John P., and Seacord, Charles L., Jr.: The Effect of Mass
    Distribution on the Lateral Stability and Control Characteristics
    of an Airplane as Determined by Tests of a Model in the Free-
    Flight Tunnel. NACA Rep. No. 769, 1943.

18. McKinney, Marion O., Jr.: Experimental Determination of the Effects
    of Dihedral, Vertical-Tail Area, and Lift Coefficient on Lateral
    Stability and Control Characteristics. NACA TN No. 1094, 1946.

19. Drake, Hubert M.: The Effect of Lateral Area on the Lateral Stability
    and Control Characteristics of an Airplane as Determined by Tests
    of a Model in the Langley Free-Flight Tunnel. NACA ARR No. L5L05,
    1946.

20. Zimmerman, Charles H.: An Analysis of Longitudinal Stability in
    Power-Off Flight with Charts for Use in Design. NACA Rep.
    No. 521, 1935.

21. Donlan, Charles J.: Some Theoretical Considerations of Longitudinal
    Stability in Power-Off Flight with Special Reference to Wind-
    Tunnel Testing. NACA ARR, Nov. 1942.

22. Lyon, H. M., Truscott, P. M., Auterson, E. I., and Whatham, J.: A
    Theoretical Analysis of Longitudinal Dynamic Stability in Gliding
    Flight. R. & M. No. 2075, British A.R.C., 1942.

23. Greenberg, Harry, and Sternfield, Leonard: A Theoretical Investigation
    of the Lateral Oscillations of an Airplane with Free Rudder with
    Special Reference to the Effect of Friction. NACA Rep. 762, 1943.

24. McKinney, Marion O., Jr., and Maggin, Bernard: Experimental Verification
    of the Rudder-Free Stability Theory for an Airplane Model Equipped
    with Rudders Having Negative Floating Tendency and Negligible
    Friction. NACA ARR No. L4J05a, 1944.

25. Maggin, Bernard: Experimental Verification of the Rudder-Free Stability
    Theory for an Airplane Model Equipped with a Rudder Having Positive
    Floating Tendencies and Various Amounts of Friction. NACA TN
    No. 1359, 1947.

26. Cohen, Doris: A Theoretical Investigation of the Rolling Oscillations
    of an Airplane with Ailerons Free. NACA Rep. No. 787, 1944.

27. Greenberg, Harry, and Sternfield, Leonard: A Theoretical Investigation
    of Longitudinal Stability of Airplanes with Free Controls Including
    Effect of Friction in Control System. NACA Rep. No. 791, 1944.

28. Phillips, William H.: A Flight Investigation of Short–Period
    Longitudinal Oscillations of an Airplane with Free Elevator.
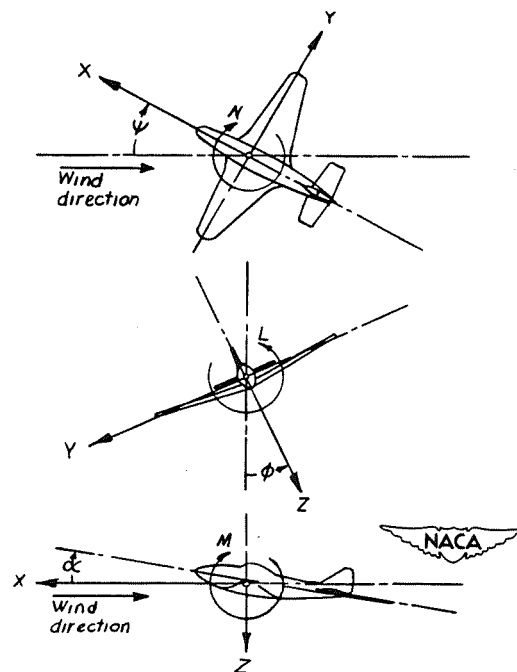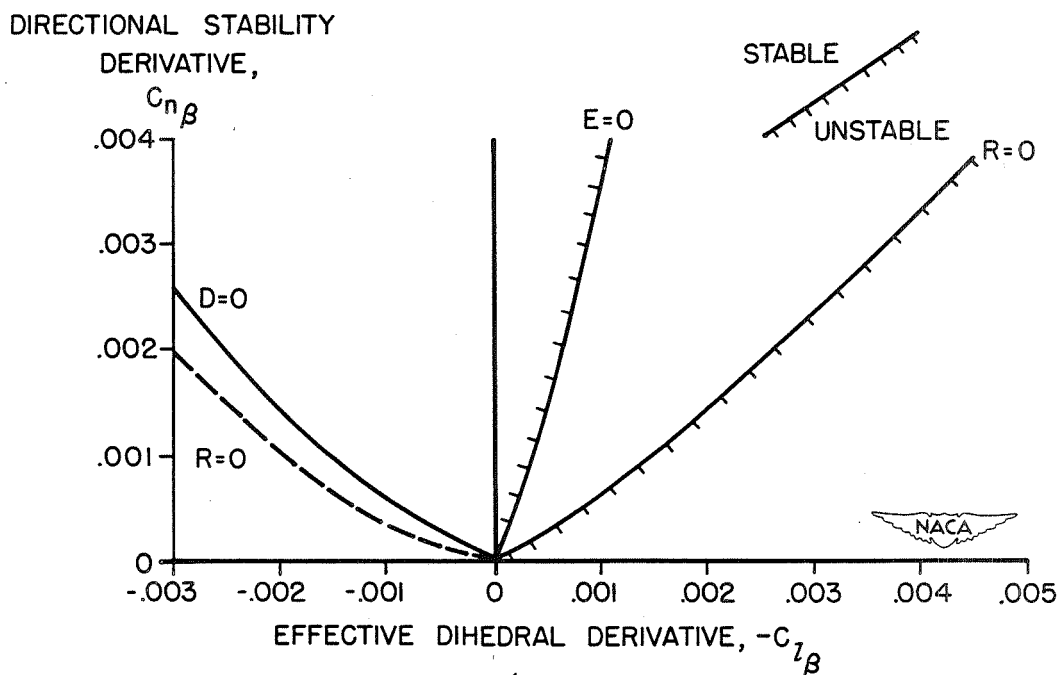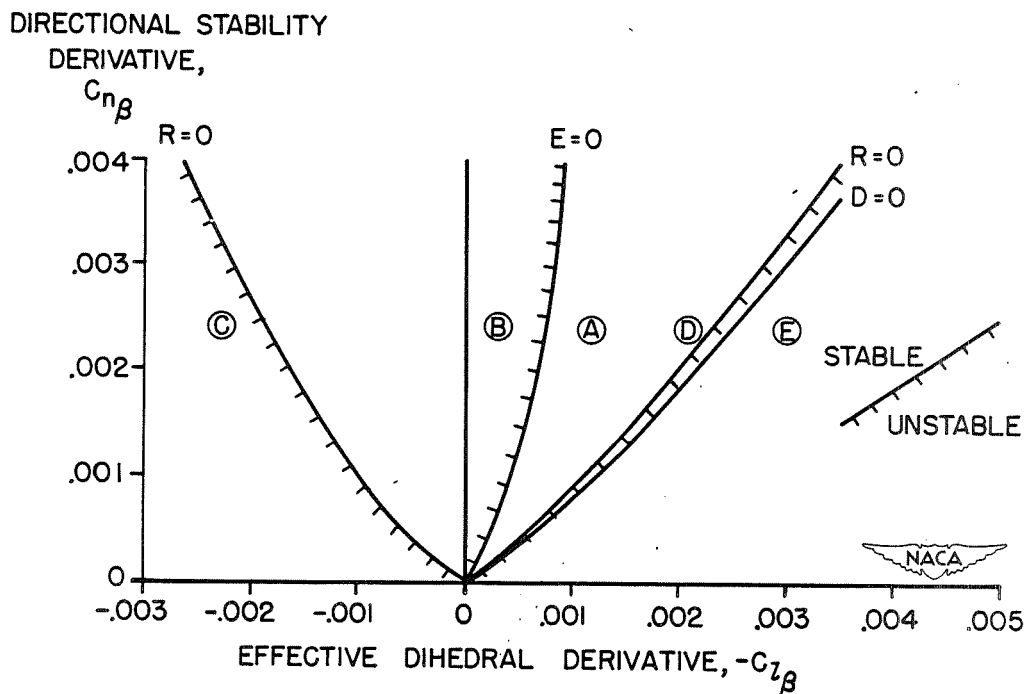   NACA ARR, May 1942.

Figure 1.- The stability system of axes. Arrows indicate positive directions of moments, forces, and control-surface deflection.

DIRECTIONAL STABILITY
DERIVATIVE,
C_{n_β}

STABLE

E=0

UNSTABLE

R=0

.004

.003

D=0

.002

.001

R=0

NACA

0

-.003   -.002   -.001   0   .001   .002   .003   .004   .005

EFFECTIVE DIHEDRAL DERIVATIVE, $-C_{l_\beta}$

(a)   The case for which only one of the two branches of the curve   R = 0   is
a boundary for neutral oscillatory stability.

DIRECTIONAL STABILITY
DERIVATIVE,
C_{n_β}

R=0

E=0

R=0

D=0

.004

.003

Ⓒ   Ⓑ   Ⓐ   Ⓓ   Ⓔ

.002

STABLE

.001

UNSTABLE

NACA

0

-.003   -.002   -.001   0   .001   .002   .003   .004   .005

EFFECTIVE DIHEDRAL DERIVATIVE, $-C_{l_\beta}$

(b)   The case for which both branches of the curve   R = 0   are boundaries
for neutral oscillatory stability.

Figure 2.-   Lateral-stability boundaries for two hypothetical high-speed-
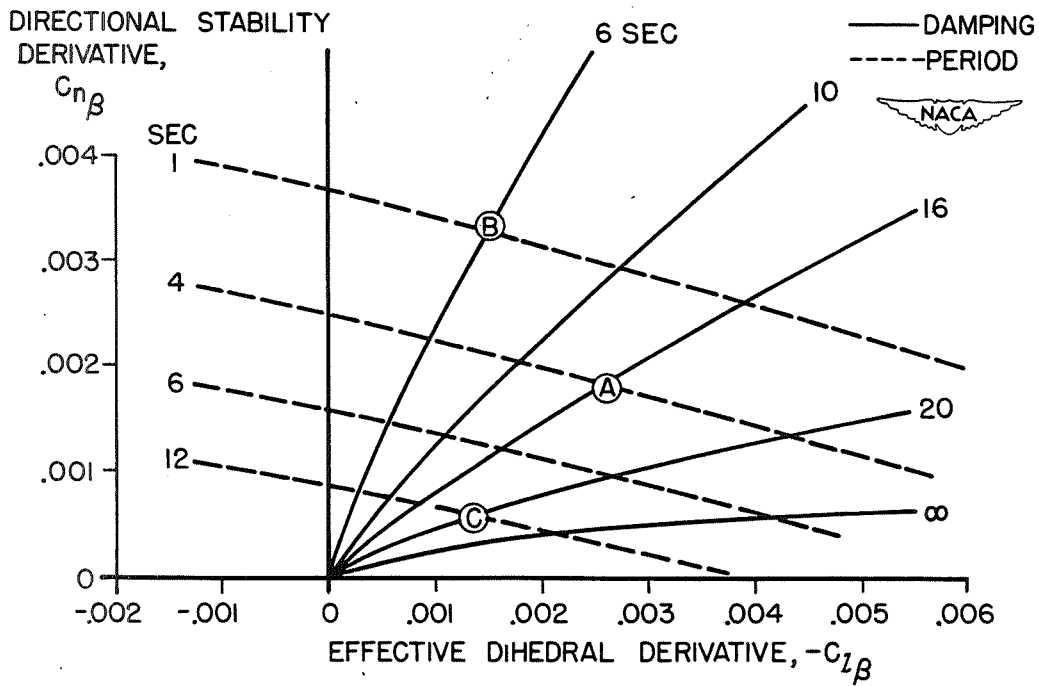airplane configurations.

248

Figure 3.- Curves of constant period and constant damping.
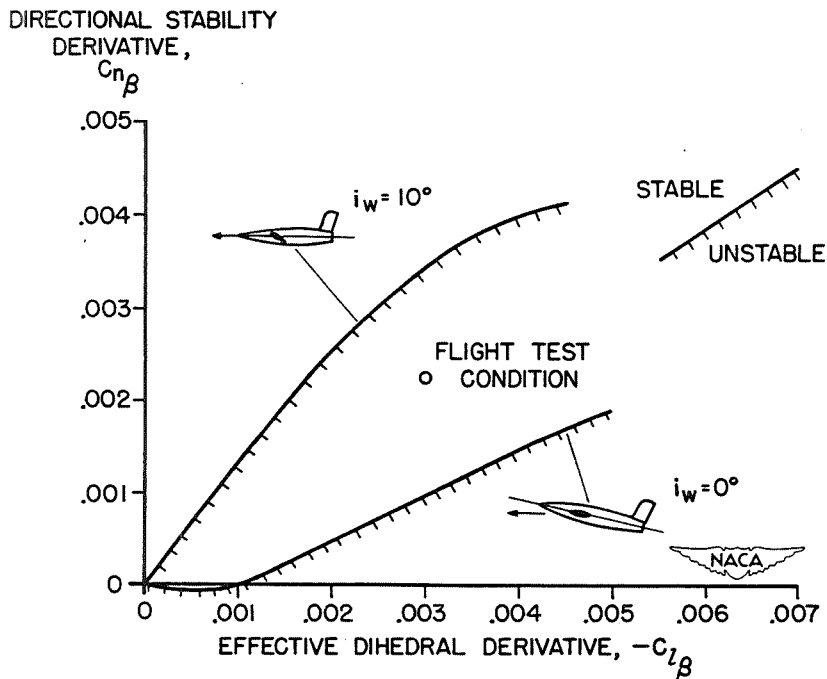

Figure 4.- Effect of wing incidence on the oscillatory stability of a model tested in the Langley free-flight tunnel.
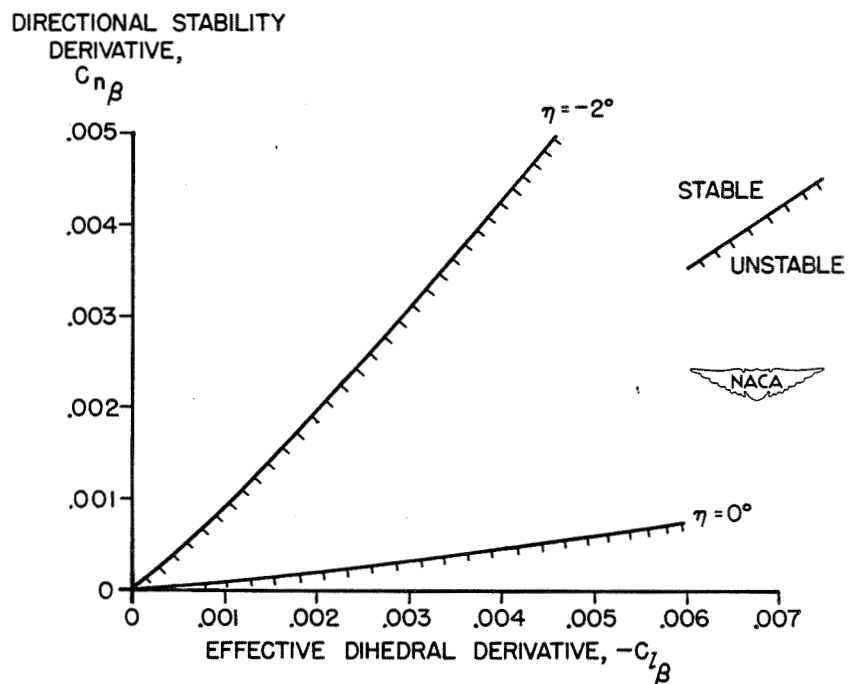
Figure 5.- Effect of the angle of attack of the principal longitudinal axis on the oscillatory-stability boundary.
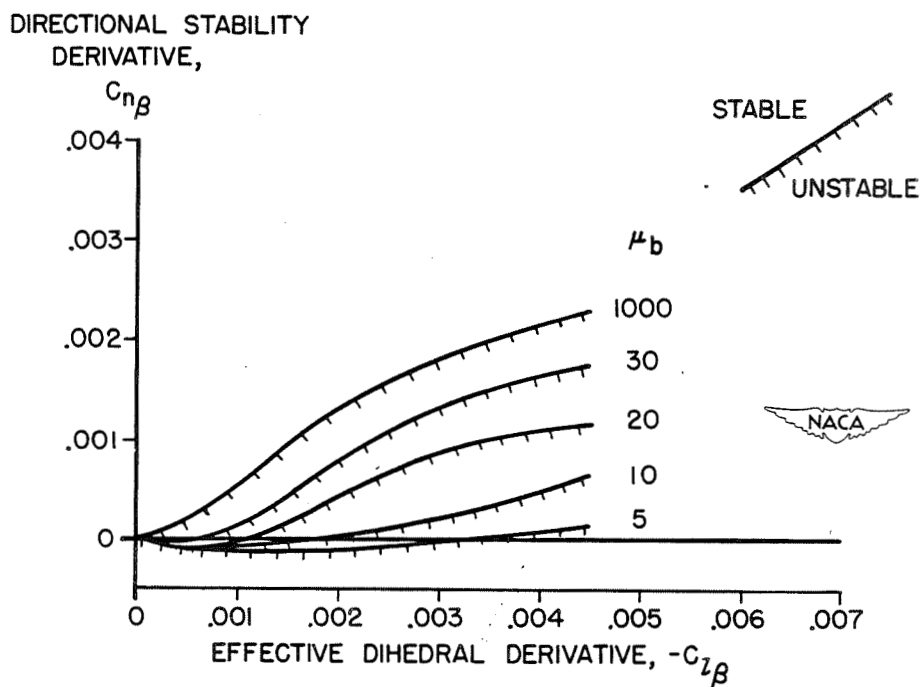

Figure 6.- Effect of the relative-density factor μ_b on the oscillatory-stability boundary.
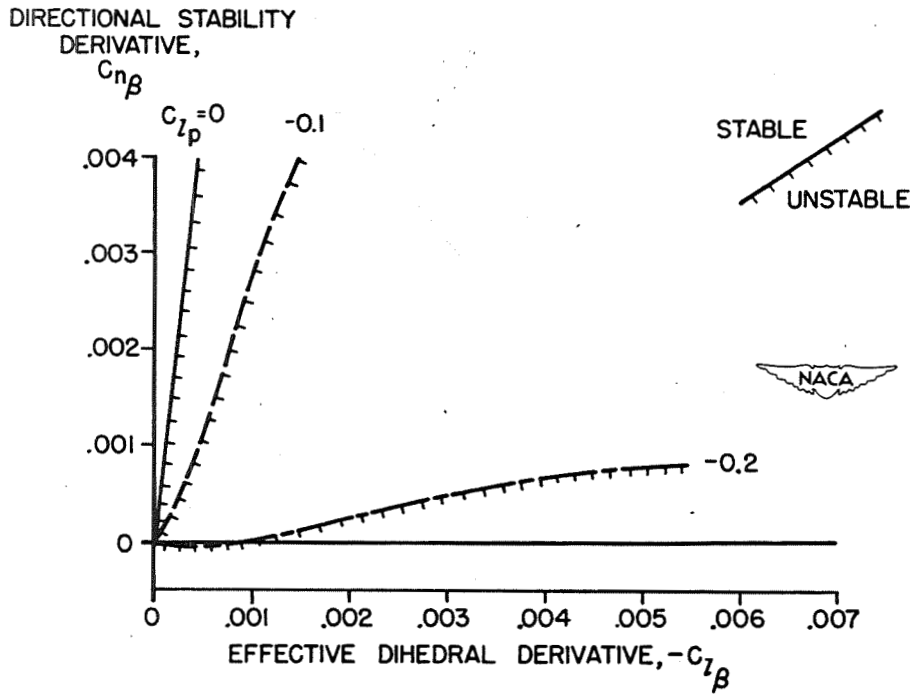
DIRECTIONAL STABILITY
DERIVATIVE,
C_{n_β}

$C_{l_p}=0$ -0.1

STABLE

UNSTABLE

.004

.003

.002

NACA

.001

-0.2

0

0   .001   .002   .003   .004   .005   .006   .007

EFFECTIVE DIHEDRAL DERIVATIVE, $-C_{l_\beta}$

Figure 7.-   Effect of damping in roll on the lateral stability of a high-
speed airplane.

R = 0   .004

FRICTION   CONSTANT
BOUNDARY   AMPLITUDE   .003

UNSTABLE

STABLE   .002

C_{h_ψ}

.001

0

DIVERGENCE
-.001

-.005   -.004   -.003   -.002   -.001   0

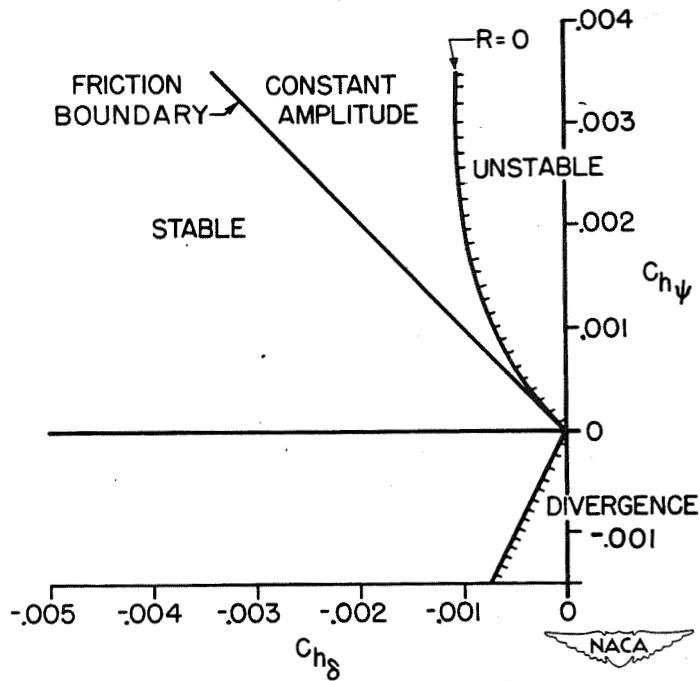C_{h_δ} NACA

Figure 8.-   Calculated rudder-free-stability boundaries for conventional
attack airplane.